HORNBLENDE GNEISSES FROM SYOWA STATION, EAST ANTARCTICA

Yoshikuni HIROI[1] and Hitoshi ONUKI[2]

[1]*Department of Earth Sciences, Faculty of Science, Chiba University, 1-33, Yayoi-cho, Chiba 260*

[2]*Department of Earth Sciences, Faculty of Science, Hirosaki University, Bunkyo-cho, Hirosaki 036*

Abstract: Pyroxene gneiss (charnockitic gneiss), local hornblende gneiss (bleached part of pyroxene gneiss), biotite schist, and pegmatite were newly analyzed chemically. The results together with the published analyses of regional hornblende gneisses and pyroxene gneisses show that regional hornblende gneisses generally have higher rock oxidation ratios and $MgO/(MgO+FeO)$ ratios than pyroxene gneisses and local hornblende gneiss, in harmony with the differences in oxide mineral assemblages and in microprobe analyses of minerals. Such differences correspond to the factors controlling the stabilities of amphiboles, and suggest that regional hornblende gneisses are the products of low granulite-facies metamorphism. The difference in mineralogy among pyroxene gneiss, local hornblende gneiss, and biotite schist may be shown by an isochemical reaction.

1. Introduction

Two kinds of hornblende gneiss occur in the granulite-facies area around Syowa Station (69°00′S, 39°35′E), East Antarctica. One shows a wide distribution as does the pyroxene gneiss (charnockite), while the other occurs as a bleached part of pyroxene gneiss along discordant pegmatite dikes. Hereafter, we will call the former regional hornblende gneiss and the latter local hornblende gneiss, respectively. KIZAKI (1964) first described local hornblende gneiss from the East Ongul Island where Syowa Station is situated, and discussed the polymetamorphic effect of the discordant pegmatite on the preexisting high-grade metamorphics. He suggested that both types of hornblende gneiss were formed from pyroxene gneiss by "granitization". This was based on his interpretation of the geologic structure of the East Ongul Island and on the observed local polymetamorphic phenomenon mentioned above. However, KANISAWA *et al.* (1979) showed that both hornblende and biotite in regional hornblende gneiss are rich in Ti and F and have characteristics of the granulite facies. Moreover, MATSUMOTO *et al.* (1982) re-examined the geologic structure of the Ongul Islands and the neighboring areas and proposed a new interpretation. In this the correlation by KIZAKI (1964) between pyroxene gneiss and the alternation of pyroxene gneiss and regional hornblende gneiss because of an antiform structure in the East Ongul Island was denied.

This paper aims to clarify the chemical difference in both rocks and minerals between regional and local hornblende gneisses around Syowa Station. It also aims to show that regional hornblende gneiss is one of the products of the granulite-facies metamorphism based on the recent experimental and theoretical studies of the stability of amphiboles and on the petrology of the high-grade metamorphic rocks around Syowa Station.

2. Geologic Setting

Syowa Station is situated on the East Ongul Island which is separated from the Prince Olav and Sôya Coasts of the Antarctic continent by the Ongul Strait about 5 km wide (Figs. 1 and 2).

The high-grade metamorphic rocks exposed along the Prince Olav and Sôya Coasts are collectively called the Lützow-Holm Complex (HIROI *et al.*, 1984), the geologic history of which is distinct from that of the neighboring Rayner Complex (Fig. 1). Recent petrologic studies of the Lützow-Holm Complex have revealed that the Prince Olav and Sôya Coasts are divided into three areas of different metamorphic grades (Fig. 1) (HIROI *et al.*, 1983b, c; SHIRAISHI *et al.*, 1984). The eastern part of the Prince Olav Coast is an amphibolite-facies area where calcium-poor amphiboles (anthophyllite, gedrite, and cummingtonite) occur characteristically (RAVICH and KAMENEV, 1975; HIROI *et al.*, 1983a, c), and the western part is a transitional area from the amphibolite to granulite facies. In the transitional area orthopyroxene occurs only sporadically in rocks of appropriate bulk chemical compositions, and gedrite is still stable (HIROI *et al.*, 1983c; SHIRAISHI *et al.*, 1984). The Sôya Coast to the southwest is a granulite-facies area, where orthopyroxene commonly occurs

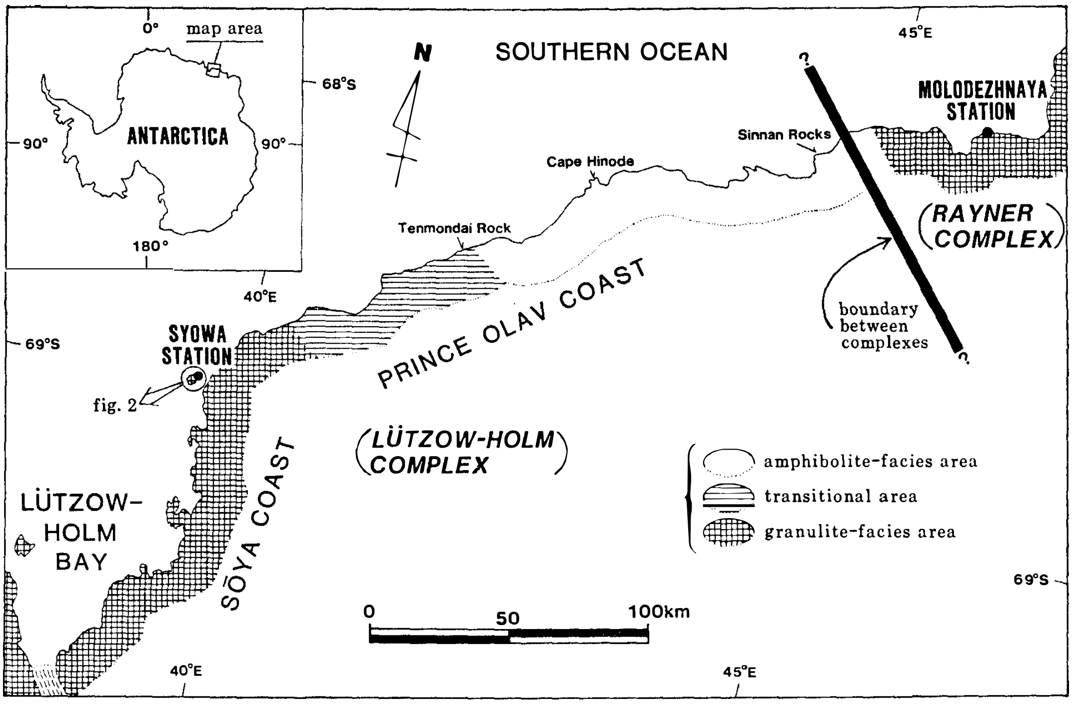

Fig. 1. Map of the Prince Olav and Sôya Coasts, showing geologic units, boundary, metamorphic facies, and the locality of Syowa Station.

in various rocks (BANNO *et al.*, 1964; KIZAKI, 1964; SUWA, 1968; YOSHIDA, 1978, 1979a, b; YOSHIDA *et al.*, 1982; SUZUKI, 1982, 1983).

Sillimanite is the stable aluminum silicate throughout the coasts, and is often associated with K-feldspar (HIROI *et al.*, 1983b, c). However, metastable kyanite occurs as inclusions in garnet and plagioclase in most of the sillimanite-bearing rocks regardless of the metamorphic grade, suggesting that the high-grade metamorphic rocks along the coasts belong to the kyanite-sillimanite type facies series. Thus progressive metamorphism of the kyanite-sillimanite type from east to west along the coasts has been established (HIROI *et al.*, 1983a, b, c; SHIRAISHI *et al.*, 1984). The Ongul Islands are located in the northeast of Lützow-Holm Bay, and are in the low-grade part of the granulite-facies area (Fig. 1).

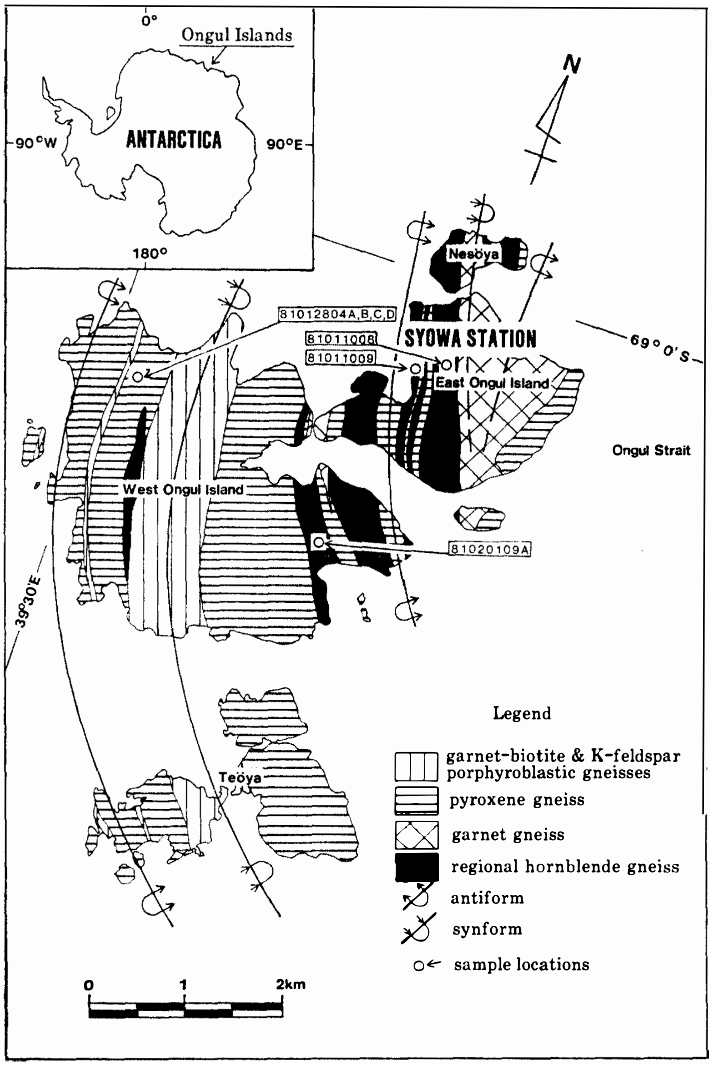

Fig. 2. Generalized geologic map of the Ongul Islands, showing major lithologies, folds, and locations of samples analyzed. This map is based on KIZAKI (1964), ISHIKAWA (1976), YANAI et al. (1974a, b, 1975a, b), MATSUMOTO et al. (1982), and field work by one of the authors (Y. H.).

The Ongul Islands are underlain mainly by pyroxene gneiss, garnet gneiss, regional hornblende gneiss, and garnet-biotite gneiss with subordinate amounts of metabasites (metamorphosed basic to ultrabasic rocks), K-feldspar porphyroblastic gneiss, granite, and pegmatite (Fig. 2). At least two stages of folding have been recognized; the earlier isoclinal folds with axial planes trending N-S and the later open folds with axial planes trending nearly E-W (ISHIKAWA, 1976; YOSHIDA, 1978; MATSUMOTO *et al.*, 1982).

The K-Ar and Rb-Sr ages of total rocks or mineral separates concentrate at about 500 Ma, indicating the heating event coeval with the Early Paleozoic granite and pegmatite activity (YANAI and UEDA, 1974), which is known over a large portion of East Antarctica (GREW, 1982). A few Rb-Sr total rock or mineral ages, however, range from 1200 to 700 Ma (MAEGOYA *et al.*, 1968; SHIRAHATA, 1983; YANAI *et al.*, 1983), dating the earlier regional metamorphism.

3. Field and Microscopic Occurrence of Hornblende Gneisses, Pyroxene Gneiss, and Biotite Schist

Mineral assemblages of the rocks described and mineral abbreviations used in this paper are given in Table 1.

Table 1. Mineral assemblages of rocks described and mineral abbreviations.

Sample number	Rock name	Minerals																
		Opx	Hb	Bi	Mus	Pl	Ksp	Sc	Qz	Il	Hm	Mt	Cc	Dol	Ap	Al	Zr	Chl
81011008	R. Hb gn.*		+	+	s**	+	+		+	+	+		s		+		+	s
81020109A	R. Hb gn.		+	+	s	+	+		+	+	+	+	s		+		+	s
81011009	R. Hb gn.		+	+	s	+	+	+	+	+	+			+	+		+	s
81012804A	Px gn***	+	+	+	s	+	+		+			+	s		+		+	s
81012804B	L. Hb gn.****		+	+	s	+	+		+	+			s		+		+	s
81012804C	Bi schist			+	s	+	+		+			+	+		+	+	+	s
81012804D	Pegmatite			+	+	+	+		+			+	s		+	+	+	s

Mineral abbreviations

Al —allanite	Hb —hornblende	Opx—orthopyroxene
Ap —apatite	Hm —hematite	Pl —plagioclase
Bi —biotite	Il —ilmenite	Qz —quartz
Cc —calcite	Ksp—K-feldspar	Sc —scapolite
Chl —chlorite	Mt —magnetite	Zr —zircon
Dol —dolomite	Mus—muscovite	

*: Regional hornblende gneiss.
**: Secondary.
***: Pyroxene gneiss.
****: Local hornblende gneiss.
Pyrite is also present in Sp. 81020109A, while pyrrhotite is an additional phase in Sp. 81012804C.

3.1. Regional hornblende gneiss

This rock occurs as layers, up to several tens of meters thick, intercalated mainly with pyroxene gneiss (Fig. 2). To the naked eye it is white, gray, or pink and is easily

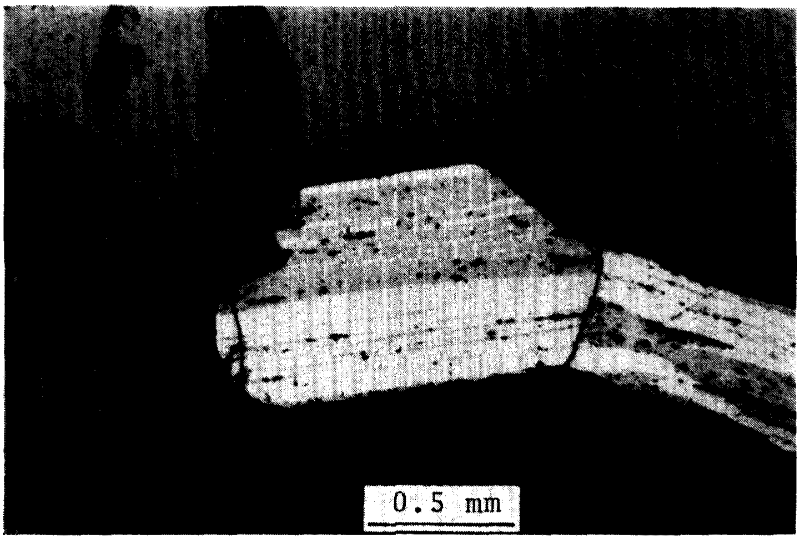

Fig. 3. Photomicrograph showing textures of ilmenite and hematite in regional hornblende gneiss.

distinguished from alternating yellow-brown pyroxene gneiss. Regional hornblende gneiss and pyroxene gneiss change gradually to each other.

Regional hornblende gneiss usually consists of hornblende, biotite, plagioclase, K-feldspar, quartz, apatite, zircon, and opaque minerals. Secondary muscovite, chlorite, and calcite are also present in small amounts. Scapolite and dolomite are additional phases in some cases. The opaque minerals are ilmenite and hematite with or without magnetite and pyrite. Ilmenite and hematite often show an intergrowth texture (Fig. 3). Hornblende is characterized by pleochroism of X′=yellow and Z′=brownish green or greenish brown. Biotite usually shows pleochroism of X′=yellow and Z′=reddish brown. Plagioclase, K-feldspar, and quartz together with smaller amounts of hornblende and biotite make up a granoblastic texture of the rocks. Plagioclase shows an antiperthitic texture. K-feldspar is highly perthitic.

3.2. *Local hornblende gneiss*

This rock occurs as a bleached part of pyroxene gneiss along pegmatite dikes (Figs. 4a, 4b). The boundary between local hornblende gneiss and pyroxene gneiss is relatively sharp, though it is winding (Fig. 4b). The gneissose structure of pyroxene gneiss, defined by the preferred orientation of mafic minerals, is continuous with that of local hornblende gneiss (Figs. 4a, 4b). However, the gneissose structure of local hornblende gneiss close to pegmatite is parallel to the dikes of pegmatite (Fig. 4c).

Local hornblende gneiss is also white, gray, or pink to the naked eye, and, therefore, is similar to the regional hornblende gneiss. The constituent minerals of local hornblende gneiss are the same as those of regional hornblende gneiss except for opaque mineral(s). The opaque mineral(s) in local hornblende gneiss is usually ilmenite with or without magnetite. Ilmenite is apparently free from hematite lamellae under the microscope. Hornblende characteristically shows pleochroism of X′=yellow and Z′=blue-green, and is often poikilitic with inclusions of quartz (Fig. 5b). Biotite is pleochroic with X′=yellow and Z′=dark brown. Plagioclase often

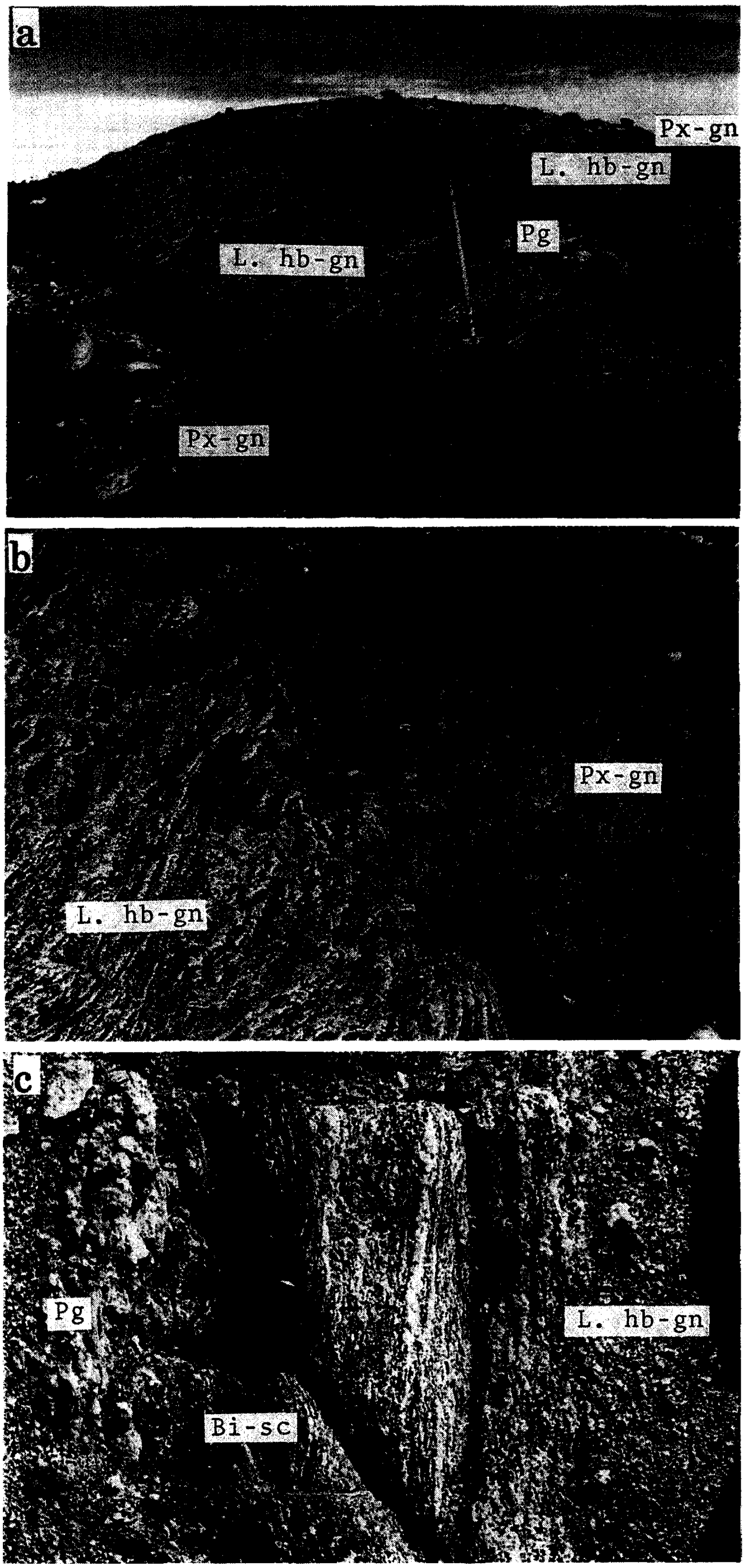

Fig. 4a. Development of local hornblende gneiss from pyroxene gneiss along pegmatite dike.

Fig. 4b. Winding and relatively sharp boundary between pyroxene gneiss and local hornblende gneiss.

Fig. 4c. Biotite schist developed between local hornblende gneiss and pegmatite. Note the schistosity of biotite schist parallel to the dike of pegmatite. The gneissose structure of local hornblende gneiss close to biotite schist is also parallel to the dike of pegmatite.

Fig. 4. Photographs showing field occurrence of pyroxene gneiss (Px-gn), local hornblende gneiss (L. hb-gn), biotite schist (Bi-sc), and pegmatite (Pg).

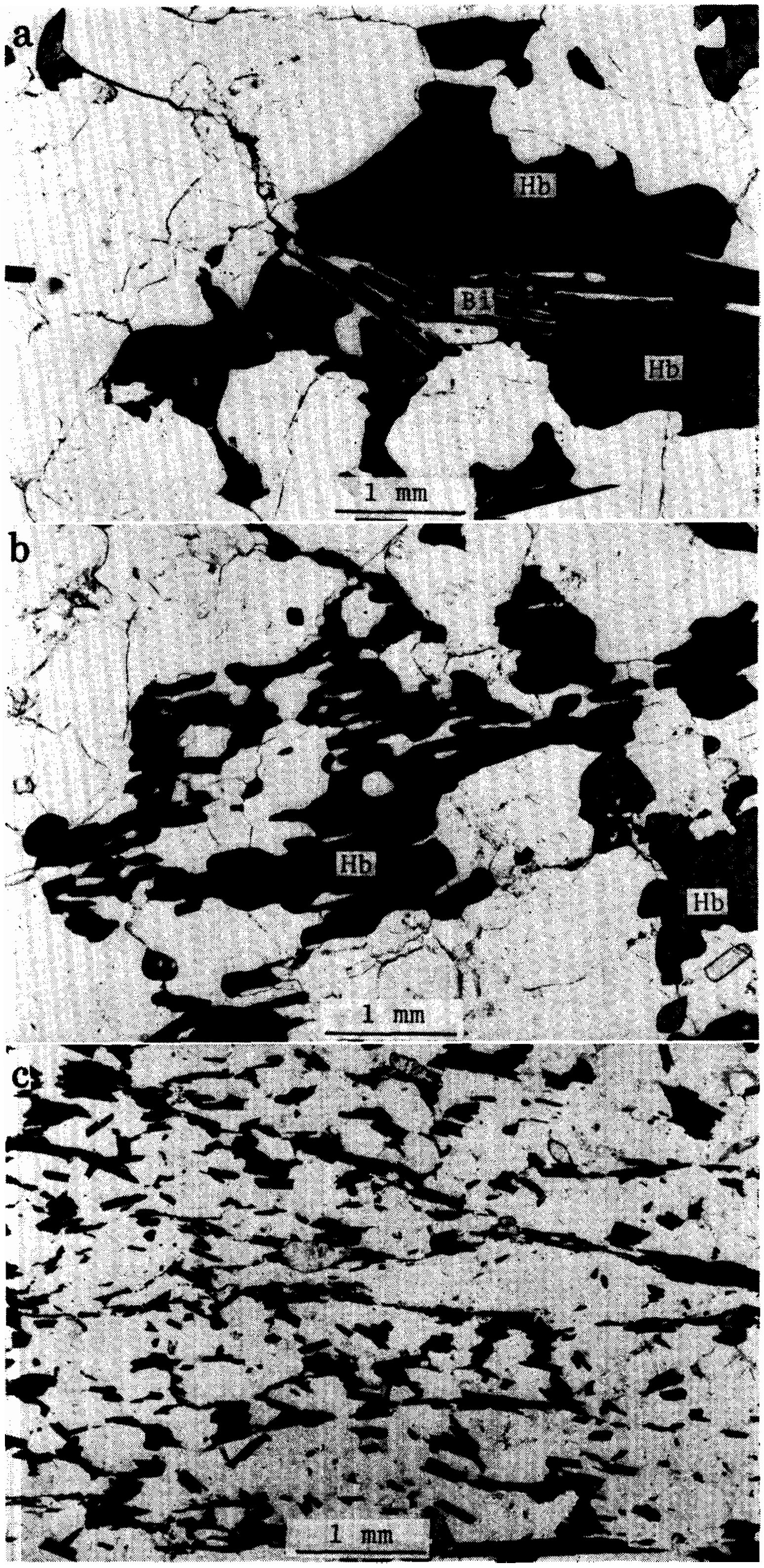

Fig. 5a. Greenish brown hornblende and dark brown biotite in pyroxene gneiss (Sp. 81012804A). One nicol.

Fig. 5b. Blue-green hornblende in local hornblende gneiss (Sp. 81012804B). Note the poikilitic texture of hornblende with inclusions of quartz. One nicol.

Fig. 5c. Dark brown biotite in biotite schist (Sp. 81012804C). One nicol.

Fig. 5. Photomicrographs showing textures of minerals in pyroxene gneiss, local hornblende gneiss, and biotite schist.

shows antiperthitic and myrmekitic textures. K-feldspar commonly shows a perthitic texture.

3.3. *Pyroxene gneiss*

Pyroxene gneiss exposed in the Ongul Islands is divided into three types, basic enderbitic, garnet-bearing enderbitic, and charnockitic, based on the petrographic characteristics (YANAI *et al.*, 1974a, b, 1975a, b). The rock often alternates with regional hornblende gneiss as layers up to several tens of meters thick. Pyroxene gneiss is characterized by the yellow-brown color due to the colored feldspars and quartz.

The analyzed specimen (81012804A) is charnockitic, being composed of orthopyroxene, hornblende, biotite, plagioclase, K-feldspar, quartz, apatite, zircon, and magnetite. Orthopyroxene occurs only in a small amount. Hornblende is pleochroic

Table 2. Bulk chemical compositions of local hornblende gneiss and associated rocks.

Sp. No.	81012804A	81012804B	81012804C	81012804D
SiO_2	61.61	64.97	64.41	69.94
TiO_2	0.92	1.02	1.13	0.86
Al_2O_3	16.34	15.48	17.12	15.02
Fe_2O_3	1.41	1.33	1.10	0.65
FeO	3.71	3.60	3.25	1.73
MnO	0.14	0.12	0.12	0.06
MgO	2.48	1.93	2.57	0.21
CaO	4.90	4.35	3.34	0.98
Na_2O	3.62	4.12	4.16	2.72
K_2O	3.93	2.45	2.29	7.46
$H_2O(+)$	0.47	0.41	0.40	0.39
$H_2O(-)$	0.04	0.03	0.03	0.02
P_2O_5	0.22	0.16	0.15	0.10
Total	99.79	99.97	100.07	100.14
Normative				
Q	11.26	18.91	19.33	22.83
Or	23.23	14.48	13.53	44.09
Ab	30.63	34.86	35.20	23.02
An	16.73	16.51	15.59	4.21
C	—	—	2.08	0.93
Di Wo	2.57	1.68	—	—
Di En	1.44	0.89	—	—
Di Fs	1.02	0.75	—	—
Hy En	4.74	3.92	6.40	0.52
Hy Fs	3.37	3.30	3.42	1.33
Mt	2.04	1.93	1.59	0.94
Il	1.75	1.94	2.15	1.63
Hm	—	—	—	—
Ap	0.51	0.37	0.35	0.23
$Mg/Mg+Fe^{2+}$	0.456	0.511	0.415	0.823
Fe^{3+}/total Fe	0.255	0.250	0.234	0.252

Analysts; M. TEZUKA and H. ONUKI.

Fig. 6a.

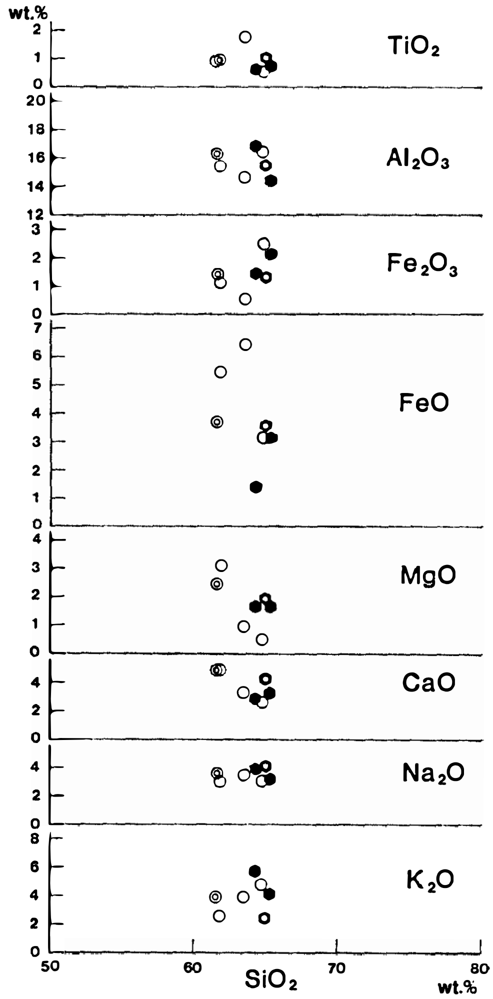

Figs. 6a, b. Diagrams showing bulk chemical compositions of pyroxene gneisses, regional hornblende gneisses, local hornblende gneiss, biotite schist, and pegmatite.

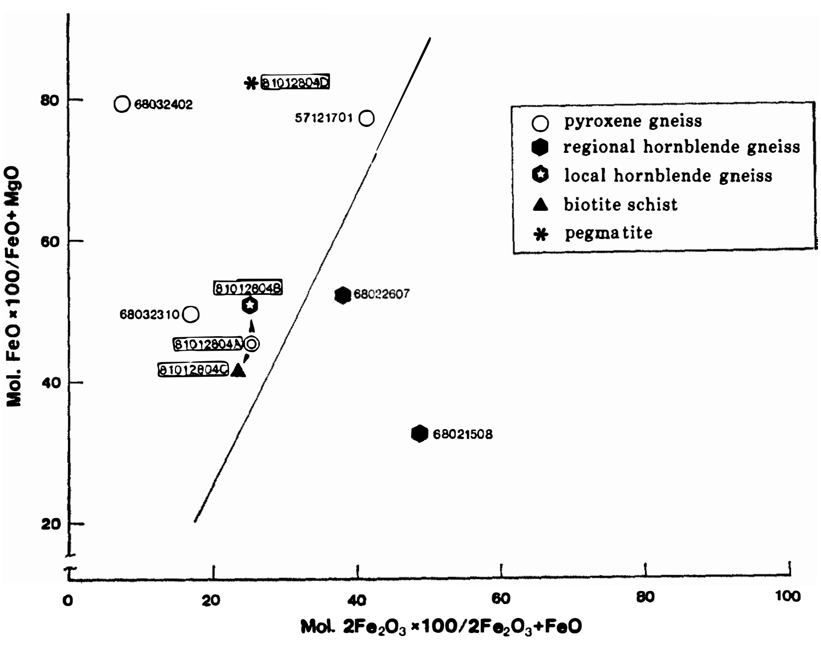

Fig. 6b.

with X′=yellow and Z′=greenish brown. Biotite sometimes shows a poikilitic texture (Fig. 5a). It is pleochroic with X′=yellow and Z′=dark brown. Plagioclase is antiperthitic, and K-feldspar is perthitic.

3.4. Biotite schist

Biotite schist occasionally occurs between local hornblende gneiss and pegmatite, and gradually changes to local hornblende gneiss (Fig. 4c). The schistosity is parallel to the dike of pegmatite (Fig. 4c). Constituent minerals are biotite, plagioclase, K-feldspar, quartz, calcite, apatite, zircon, allanite, and magnetite. K-feldspar occurs only in a small amount as an interstitial mineral among plagioclase and quartz grains. Biotite shows pleochroism of X′=yellow and Z′=deep brown. Plagioclase is sometimes porphyroblastic, and is usually free from K-feldspar lamellae.

4. Bulk Rock Compositions of Hornblende Gneisses, Pyroxene Gneisses, and Biotite Schist

One specimen of local hornblende gneiss (81012804B) together with specimens of neighboring pyroxene gneiss, biotite schist, and pegmatite (81012804A, 81012804C, and 81012804D) were analyzed by means of conventional wet chemical analysis. The results are listed in Table 2. The following may be noted when these analyses are compared with published analyses of regional hornblende gneisses and pyroxene gneisses (reviewed by YOSHIDA (1978)).

(1) In general, the rock oxidation ratios (CHINNER, 1960) of regional hornblende gneisses are higher than those of pyroxene gneisses and local hornblende gneiss (Fig. 6b).

(2) Pyroxene gneisses are usually more FeO-rich than regional hornblende gneisses (see Fig. 6a). MgO contents of pyroxene gneisses, on the other hand, are similar to those of regional hornblende gneisses (Fig. 6a). Therefore, the FeO/(MgO+FeO)

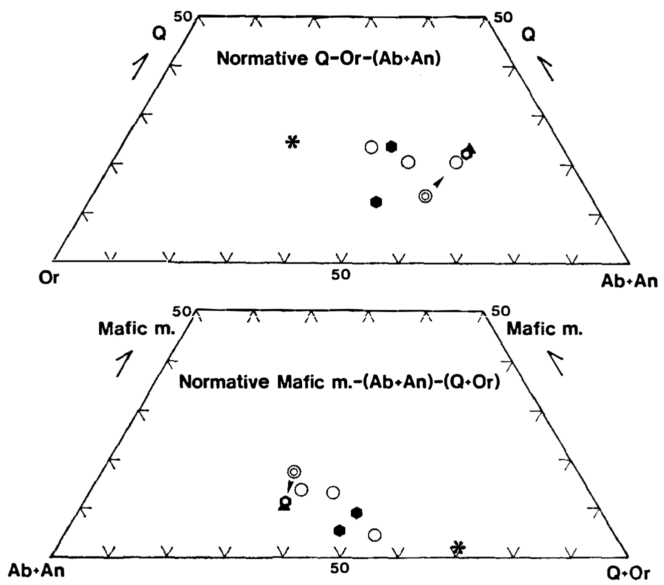

Fig. 7. Diagrams showing normative minerals of pyroxene gneisses, regional hornblende gneisses, local hornblende gneiss, biotite schist, and pegmatite. Symbols are the same as in Fig. 6.

ratios of pyroxene gneisses are higher than those of regional hornblende gneisses (Fig. 6b).

(3) Local hornblende gneiss and associated biotite schist are close to the neighboring pyroxene gneiss in chemical composition (Table 2 and Fig. 7), though local hornblende gneiss and biotite schist are slightly poorer in K_2O than neighboring pyroxene gneiss and the CaO content decreases from the pyroxene gneiss to biotite schist (Table 2).

5. Mineral Chemistry

Electron microprobe analysis of minerals was performed using JEOL-733 under such conditions as an acceleration voltage of 15 kV, beam currents of 0.012–0.015 μA, and a beam diameter of 3 μm. Generally, several grains of each mineral per specimen and two or more points per grain were analyzed. Representative analyses of minerals

Table 3. Representative microprobe analyses of minerals in regional hornblende gneiss (Sp. 81011008).

Mineral	Hb	Bi	Pl	Ksp	Hm*	Il*
SiO_2	40.49	35.82	60.73	64.94	0.00	0.00
TiO_2	2.32	5.79	0.00	0.07	10.69	46.80
Al_2O_3	10.53	13.45	24.71	18.57	0.07	0.00
Cr_2O_3	0.09	0.00	0.02	0.02	0.17	0.05
Fe_2O_3**					78.89	10.12
FeO**					9.60	42.02
FeO***	16.68	17.67	0.10	0.08		
MnO	0.36	0.24	0.05	0.01	0.07	0.84
MgO	10.74	12.64	0.00	0.00	0.05	0.41
CaO	11.51	0.01	5.66	0.15	0.00	0.00
Na_2O	1.97	0.04	8.27	3.24	0.00	0.00
K_2O	1.74	9.35	0.31	11.71	0.00	0.00
Total	96.43	95.01	99.85	98.79	99.54	100.30
O	23	22	32	32	6	8
Si	6.259	5.473	10.822	11.965	0.000	0.000
Al	1.918	2.422	5.190	4.033	0.004	0.000
Cr	0.011	0.000	0.003	0.003	0.007	0.002
Fe^{3+}**					3.135	0.386
Fe^{2+}**					0.424	1.784
Ti	0.270	0.665	0.000	0.010	0.425	1.784
Fe***	2.156	2.259	0.015	0.013		
Mn	0.047	0.031	0.007	0.001	0.003	0.036
Mg	2.474	2.880	0.000	0.000	0.004	0.031
Ca	1.907	0.002	1.081	0.029	0.000	0.000
Na	0.591	0.011	2.856	1.156	0.000	0.000
K	0.342	1.823	0.071	2.753	0.000	0.000
Mg/Mg+Fe***	0.534	0.560				
Ab %			71.26	29.35		

* Intergrowth. ** Calculated by assuming Ti=Fe^{2+}. *** Total Fe.

Table 4. Representative microprobe analyses of minerals in regional hornblende gneiss (Sp. 81020109A).

Mineral	Hb	Bi	Pl	Ksp	Mt	Hm*	Il*
SiO_2	41.01	36.61	62.37	64.58	0.00	0.00	0.00
TiO_2	2.42	5.63	0.06	0.03	0.09	10.92	46.83
Al_2O_3	9.89	13.45	23.76	18.67	0.30	0.12	0.03
Cr_2O_3	0.01	0.00	0.02	0.03	0.12	0.19	0.03
Fe_2O_3**					67.85	78.59	9.37
FeO**					30.53	9.83	42.12
FeO***	16.94	16.21	0.06	0.01			
MnO	0.49	0.22	0.00	0.07	0.00	0.00	0.40
MgO	10.58	13.19	0.00	0.00	0.07	0.08	0.74
CaO	11.46	0.00	4.86	0.06	0.00	0.00	0.00
Na_2O	1.96	0.05	9.03	1.83	0.00	0.00	0.00
K_2O	1.50	9.32	0.17	14.07	0.00	0.00	0.00
Total	96.26	94.68	100.33	99.35	98.96	99.73	99.52
O	23	22	32	32	8	6	6
Si	6.345	5.560	11.027	11.938	0.000	0.000	0.000
Al	1.804	2.408	4.952	4.068	0.005	0.007	0.002
Cr	0.002	0.001	0.003	0.004	0.007	0.008	0.001
Fe^{3+}**					3.964	3.115	0.359
Fe^{2+}**					1.982	0.433	1.795
Ti	0.282	0.643	0.008	0.004	0.005	0.433	1.794
Fe***	2.192	2.059	0.009	0.001			
Mn	0.064	0.028	0.000	0.011	0.000	0.000	0.017
Mg	2.439	2.987	0.000	0.000	0.008	0.006	0.056
Ca	1.900	0.000	0.921	0.011	0.000	0.000	0.000
Na	0.589	0.014	3.095	0.656	0.000	0.000	0.000
K	0.297	1.805	0.038	3.318	0.000	0.000	0.000
Mg/Mg+Fe***	0.527	0.592					
Ab %			76.35	16.46			

* Intergrowth. ** Calculated by assuming $2Fe^{2+}=Fe^{3+}$ for magnetite and $Ti=Fe^{2+}$ for hematite and ilmenite. *** Total Fe.

in each specimen are listed in Tables 3–7.

5.1. Hornblende

Hornblendes in regional hornblende gneisses and pyroxene gneiss are rich in Ti, containing more than 2.0 wt% TiO_2, in comparison with that in local hornblende gneiss which contains less than 2 wt% TiO_2. The Mg/(Mg+total Fe) ratios of hornblendes in regional hornblende gneisses are usualy higher than those in pyroxene gneiss and associated local hornblende gneiss, in harmony with the difference in the MgO/(MgO+FeO) ratios of host rocks mentioned above. If we take the difference in the rock oxidation ratios between regional hornblende gneiss and pyroxene gneiss into account, the difference in the ratios is greater.

It is worthy to note that chemical features of hornblende in local hornblende gneiss are similar to those in the neighboring pyroxene gneiss except for the Ti content.

Table 5. Representative microprobe analyses of minerals in scapolite-bearing regional hornblende gneiss (Sp. 81011009).

Mineral	Hb	Bi	Pl	Ksp	Sc	Dol	Hm*
SiO_2	40.56	36.21	61.26	63.66	50.02	0.00	0.00
TiO_2	2.07	4.98	0.04	0.06	0.00	0.00	11.50
Al_2O_3	10.99	13.37	24.28	18.26	24.03	0.00	0.11
Cr_2O_3	0.02	0.00	0.00	0.00	0.00	0.00	0.11
Fe_2O_3**							77.74
FeO**							10.34
FeO***	17.33	16.62	0.00	0.13	0.04	5.79	
MnO	0.23	0.00	0.00	0.01	0.05	0.84	0.05
MgO	10.33	13.39	0.02	0.00	0.02	16.75	0.05
CaO	11.33	0.00	5.78	0.12	11.92	28.92	0.00
Na_2O	1.83	0.09	8.38	1.67	6.51	0.00	0.00
K_2O	1.91	9.39	0.25	14.03	0.70	0.00	0.00
Total	96.60	94.05	100.01	97.94	93.29	52.30	99.93
O	23	22	32	32	Si+Al=12	6	6
Si	6.265	5.551	10.890	11.948	7.661	0.000	0.000
Al	2.001	2.416	5.087	4.038	4.339	0.000	0.007
Cr	0.002	0.000	0.000	0.000	0.000	0.000	0.005
Fe^{3+}**							3.075
Fe^{2+}**							0.455
Ti	0.240	0.575	0.006	0.009	0.000	0.000	0.455
Fe***	2.239	2.131	0.000	0.020	0.005	0.472	
Mn	0.030	0.000	0.000	0.002	0.006	0.069	0.002
Mg	2.380	3.061	0.004	0.000	0.003	2.435	0.004
Ca	1.875	0.000	1.101	0.024	1.956	3.023	0.000
Na	0.548	0.028	2.888	0.609	1.932	0.001	0.000
K	0.376	1.837	0.056	3.359	0.137	0.000	0.000
Mg/Mg+Fe***	0.515	0.590					
Ab %			71.40	15.25			

* Intergrowth with ilmenite. ** Calculated by assuming $Ti=Fe^{2+}$. *** Total Fe.

Therefore, the difference in axial color of hornblende mentioned above can be attributed to the difference in the Ti content of hornblende.

As shown in Fig. 8, all hornblendes are close to pargasite endmember in composition.

5.2. *Biotite*

Like the case of hornblende, biotites in regional hornblende gneisses and pyroxene gneiss are rich in Ti, containing about 5 wt% TiO_2, in comparision with those in local hornblende gneiss and associated biotite schist which contain less than 4.5 wt% TiO_2. The Mg/(Mg+total Fe) ratios of biotites in regional hornblende gneisses are higher than those in pyroxene gneiss and associated local hornblende gneiss, in harmony with the difference in the MgO/(MgO+FeO) ratios of host rocks mentioned above. As shown in Tables 3–5, the Al contents of biotites in regional hornblende gneisses are insufficient to fulfill the tetrahedrally coordinated cation sites, suggesting that these

Table 6. Representative microprobe analyses of minerals in pyroxene gneiss (Sp. 81012804A).

Mineral	Opx	Hb	Bi	Pl	Ksp	Mt
SiO_2	50.83	41.37	36.01	60.16	65.10	0.10
TiO_2	0.12	2.70	5.59	0.02	0.04	0.19
Al_2O_3	0.77	11.16	13.73	24.84	18.45	0.32
Cr_2O_3	0.00	0.00	0.01	0.00	0.00	0.11
Fe_2O_3*						68.36
FeO*						30.76
FeO**	29.85	18.82	19.90	0.12	0.10	
MnO	1.55	0.32	0.11	0.11	0.00	0.07
MgO	16.58	8.88	11.02	0.01	0.00	0.02
CaO	0.66	11.31	0.00	6.75	0.12	0.00
Na_2O	0.00	1.65	0.05	7.75	2.69	0.00
K_2O	0.00	1.62	9.04	0.34	12.25	0.00
Total	100.36	97.83	95.46	100.10	98.75	99.93
O	6	23	22	32	32	8
Si	1.969	6.321	5.513	10.729	12.007	0.008
Al	0.035	2.009	2.477	5.220	4.010	0.029
Cr	0.000	0.000	0.001	0.000	0.000	0.007
Fe^{3+}*						3.951
Fe^{2+}*						1.976
Ti	0.004	0.311	0.644	0.003	0.005	0.011
Fe**	0.967	2.405	2.548	0.018	0.015	
Mn	0.051	0.041	0.014	0.017	0.000	0.005
Mg	0.957	2.022	2.516	0.001	0.000	0.002
Ca	0.028	1.852	0.000	1.291	0.024	0.000
Na	0.000	0.490	0.013	2.679	0.961	0.000
K	0.000	0.316	1.766	0.077	2.881	0.000
Mg/Mg+Fe**	0.498	0.457	0.497			
Ab %				66.21	24.84	

* Calculated by assuming $2Fe^{2+}=Fe^{3+}$. ** Total Fe.

biotites contain ferric iron. This is in good agreement with the fact that regional hornblende gneisses have higher rock oxidation ratios than pyroxene gneisses and local hornblende gneiss. The Mg/(Mg+total Fe) ratio of biotite in biotite schist is still lower than those in adjacent local hornblende gneiss and pyroxene gneiss.

5.3. Ilmenite and hematite

Ilmenite and hematite in regional hornblende gneisses are usually intergrown with each other as shown in Fig. 3. Moreover, ilmenite always contains hematite lamellae, and *vice versa.* Thus, it seems highly probable that the ilmenite-hematite intergrowths were once homogeneous hemoilmenite or ilmenohematite grains. On the other hand, ilmenite in local hornblende gneiss is apparently free from hematite lamellae under the microscope, though microprobe analysis shows that it does contain a hematite component.

Table 7. Representative microprobe analyses of minerals in local hornblende gneiss (Sp. 81012804B) and associated biotite schist (Sp. 81012804C).

Specimen	81012804B					81012804C		
Mineral	Hb	Bi	Pl	Ksp	Il	Bi	Pl	Mt
SiO_2	41.00	36.15	59.62	64.65	0.01	35.88	60.13	0.00
TiO_2	1.94	4.39	0.03	0.04	46.53	3.84	0.00	0.04
Al_2O_3	11.08	14.24	25.50	18.59	0.01	14.99	24.42	0.07
Cr_2O_3	0.01	0.00	0.00	0.01	0.02	0.04	0.02	0.11
Fe_2O_3*					10.58			69.09
FeO*					41.85			31.09
FeO**	19.39	20.27	0.17	0.09		20.43	0.09	
MnO	0.34	0.26	0.07	0.06	1.77	0.28	0.00	0.00
MgO	9.02	11.04	0.00	0.00	0.21	9.85	0.01	0.02
CaO	11.37	0.00	7.00	0.08	0.00	0.01	6.07	0.00
Na_2O	1.59	0.00	7.67	1.46	0.00	0.02	8.15	0.00
K_2O	1.64	9.38	0.33	14.45	0.00	9.16	0.14	0.00
Total	97.38	95.73	100.39	99.43	100.98	94.50	99.03	100.42
O	23	22	32	32	6	22	32	8
Si	6.320	5.535	10.617	11.952	0.001	5.560	10.807	0.000
Al	2.012	2.571	5.351	4.051	0.001	2.738	5.173	0.006
Cr	0.001	0.000	0.000	0.001	0.001	0.005	0.003	0.007
Fe^{3+}*					0.402			3.987
Fe^{2+}*					1.768			1.994
Ti	0.225	0.505	0.004	0.005	1.768	0.447	0.000	0.002
Fe**	2.499	2.595	0.025	0.014		2.648	0.014	
Mn	0.044	0.034	0.011	0.010	0.076	0.037	0.000	0.000
Mg	2.072	2.519	0.000	0.000	0.016	2.277	0.002	0.002
Ca	1.877	0.000	1.336	0.016	0.000	0.001	1.169	0.000
Na	0.474	0.000	2.647	0.524	0.000	0.007	2.841	0.000
K	0.322	1.832	0.074	3.407	0.000	1.810	0.032	0.000
Mg/Mg+Fe**	0.453	0.493				0.462		
Ab %			65.24	13.28			70.28	

* Calculated by assuming $Ti=Fe^{2+}$ for ilmenite and $2Fe^{2+}=Fe^{3+}$ for magnetite. ** Total Fe.

5.4. Other minerals

Orthopyroxene in the analyzed pyroxene gneiss is ferrohypersthene poor in Al.

Plagioclase in regional bornblende gneisses is usually oligoclase, while it is andesine in pyroxene gneiss and local hornblende gneiss. However, plagioclase in biotite schist is slightly more Na-rich than those in associated local hornblende gneiss and pyroxene gneiss.

6. Discussion

6.1. Polymetamorphic effect of pegmatite

KIZAKI (1964) first reported the polymetamorphic effect of discordant pegmatite on the preexisting granulite-facies rocks, as mentioned above. Later GREW (1978) described similar phenomena of recrystallization of pyroxene-bearing gneisses under

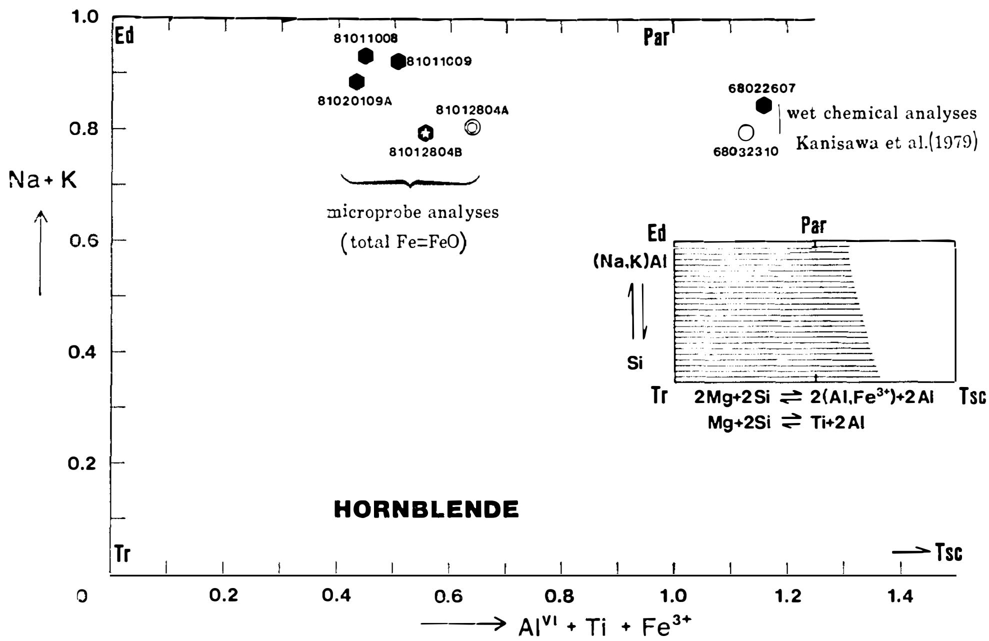

Fig. 8. Diagram showing chemical compositions of hornblendes in regional and local hornblende gneisses as well as in pyroxene gneisses. Symbols are the same as in Fig. 6.

amphibolite-facies conditions at the time of the emplacement of granite and pegmatite around Molodezhnaya Station. He showed that the resultant products are not only bleached gneisses but also blastomylonite and metasomatic scapolite. Recently HIROI *et al.* (1983b, c) showed that andalusite in kyanite-sillimanite-bearing gneisses from the Prince Olav Coast is a product of the thermal metamorphism by the granite and pegmatite, as mentioned above. Such recent studies suggest that the polymetamorphic effect of the granite and pegmatite on the preexisting high-grade metamorphics includes deformation and metasomatism under the low-pressure amphibolite-facies conditions.

In the study area the development of biotite schist with schistosity parallel to the pegmatite dike seems to suggest that deformation and metasomatism took place simultaneously at the time of the emplacement of pegmatite. However, as shown in Table 2 and Figs. 6a, 6b, and 7, major elements except for H_2O do not seem to have moved when the biotite schist and local hornblende gneiss were formed from the neighboring pyroxene gneiss. The small differences in bulk chemical composition among pyroxene gneiss, local hornblende gneiss, and biotite schist in Table 2 may be ascribed to the sampling.

The marked differences between local hornblende gneiss and adjacent pyroxene gneiss are (1) in the presence or absence of orthopyroxene, magnetite, and ilmenite, and (2) in the Ti content of hornblende and biotite. These can be shown by the next reaction.

$$\text{Opx}+\text{Ti-rich Hb}+\text{Ti-rich Bi}+\text{Pl}+\text{Ksp}+\text{Mt}+H_2O$$
$$=\text{Ti-poor Hb}+\text{Ti-poor Bi}+\text{Pl}+\text{Ksp}+\text{Qz}+\text{Il}\,.$$

The differences between local hornblende gneiss and adjacent biotite schist are (1) in the presence or absence of hornblende, ilmenite, magnetite, and calcite, (2) in the modal amounts of feldspars and quartz, especially K-feldspar, and (3) in the chemical compositions of biotite and plagioclase. These may be shown by the next reaction.

$$\text{Hb}+\text{more Mg-rich Bi}+\text{more Ca-rich Pl}+\text{Ksp}+\text{Qz}+\text{Il}+H_2O+CO_2$$
$$=\text{more Fe-rich Bi}+\text{more Na-rich Pl}+\text{Cc}+\text{Mt}.$$

6.2. Origin of regional hornblende gneiss

Regional hornblende gneisses differ from alternating pyroxene gneisses in bulk chemical composition, as shown in Fig. 6b. Regional hornblende gneisses have higher rock oxidation ratios and higher MgO/(MgO+FeO) ratios than pyroxene gneisses. In harmony, hornblendes and biotites in regional hornblende gneisses have higher Mg/(Mg+total Fe) ratios than those in pyroxene gneisses. Recent experimental and theoretical studies about the stability of amphiboles have revealed the following points (reviewed by MIYASHIRO (1973) and GILBERT *et al.* (1982)).

(1) Mg-rich phases are stable to much higher temperatures than Fe^{2+}-rich ones.

(2) Fe^{3+}-rich phases are stable to higher temperatures than Al-rich ones.

Thus, the hornblendes in the regional hornblende gneisses are stable to higher temperatures than those in pyroxene gneisses. This, in turn, suggests that the hornblendes in the pyroxene gneisses have reacted to form orthopyroxene, while those in regional hornblende gneisses did not, during the prograde recrystallization of the rocks up to the low granulite facies. In addition, the biotites in the pyroxene gneisses may also have reacted to produce orthopyroxene. As mentioned above, KANISAWA *et al.* (1979) showed that hornblende and biotite in regional hornblende gneiss are rich in Ti and F just like those in pyroxene gneiss. Therefore, it is safely concluded that the regional hornblende gneisses were stable during the low granulite-facies metamorphism as the products of prograde recrystallization of the rocks.

7. Conclusion

Two kinds of hornblende gneiss, regional and local, in the granulite-facies area around Syowa Station differ from each other in both bulk chemical composition and mineral composition. Regional hornblende gneisses have higher MgO/(MgO+FeO) and Fe(3+)/total Fe ratios than local hornblende gneiss. Such differences correspond to the factors controlling the stabilities of amphiboles. Therefore, it is concluded that the regional hornblende gneisses were stable during the granulite-facies metamorphism as the products of prograde recrystallization of the rocks.

Acknowledgments

We would like to express our sincere thanks to Miss M. Tezuka for the chemical analysis. We also deeply appreciate the kind help of Messrs. H. KOJIMA and Y. MOTOYOSHI in the microprobe analysis. Our hearty thanks are due to Dr. A. GRAHAM for his kind correction of our English.

References

BANNO, S., TATSUMI, T., OGURA, Y. and KATSURA, T. (1964): Petrographic studies on the rocks from the area around Lützow-Holmbukta. Antarctic Geology, ed. by R. J. ADIE. Amsterdam, North-Holland, 405–414.

CHINNER, G. A. (1960): Pelitic gneisses with varying ferrous/ferric ratios from Glen Clova, Angus, Scotland. J. Petrol., **1**, 178–217.

GILBERT, M. C., HELZ, R. T., POPP, R. K. and SPEAR, F. S. (1982): Experimental studies of amphibole stability. Amphibole; Petrology and Experimental Phase Relations, ed. by D. R. VEBLEN and P. H. RIBBE. Washington, D. C., Mineral. Soc. Am., 229–353 (Review in Mineralogy, Vol. 9B).

GREW, E. S. (1978): Precambrian basement at Molodezhnaya Station, East Antarctica. Geol. Soc. Am. Bull., **89**, 801–837.

GREW, E. S. (1982): The Antarctic Margin. The Ocean Basins and Margins, Vol. 6, ed. by A. E. M. NAIRN and F. G. STEHLI. New York, Plenum Press, 697–755.

HIROI, Y., SHIRAISHI, K. and YOSHIDA, Y. (1983a): Geological map of Sinnan Rocks, Antarctica. Antarct. Geol. Map Ser., Sheet 14 (with explanatory text 7p.). Tokyo, Natl Inst. Polar Res.

HIROI, Y., SHIRAISHI, K., YANAI, K. and KIZAKI, K. (1983b): Aluminum silicates in the Prince Olav and Sôya Coasts, East Antarctica. Mem. Natl Inst. Polar Res., Spec. Issue, **28**, 115–131.

HIROI, Y., SHIRAISHI, K., NAKAI, Y., KANO, T. and YOSHIKURA, S. (1983c): Geology and petrology of Prince Olav Coast, East Antarctica. Antarctic Earth Science, ed. by R. L. OLIVER *et al.* Canberra, Aust. Acad. Sci., 32–35.

HIROI, Y., SHIRAISHI, K., MOTOYOSHI, Y. and YANAI, K. (1984): Syowa Kiti shûhen ni bunpu suru genseidai henseiganrui no keisei ni taisuru purêto tekutonikku moderu (Plate tectonic model of the development of the Proterozoic metamorphics in the area around Syowa Station). Dai-5-kai Nankyoku Chigaku Shinpojiumu Puroguramu · Kôen Yôshi (Program · Abstr. 5th Symp. Antarct. Geosci.), Tokyo, Natl Inst. Polar Res., 42–43.

ISHIKAWA, T. (1976): Superimposed folding of the Precambrian metamorphic rocks of the Lützow-Holm Bay region, East Antarctica. JARE Sci. Rep., Ser. C (Earth Sci.), **9**, 41 p.

KANISAWA, S., ONUKI, H. and YANAI, K. (1979): Chemical characteristics of biotites and hornblendes from metamorphic rocks around Lützow-Holmbukta, East Antarctica. Mem. Natl Inst. Polar Res., Spec. Issue, **14**, 153–163.

KIZAKI, K. (1964): Tectonics and petrography of the East Ongul Island, Lützow-Holm Bukt, East Antarctica. JARE Sci. Rep., Ser. C (Geol.), **2**, 24 p.

MAEGOYA, T., NOHDA, S. and HAYASE, I. (1968): Rb-Sr dating of the gneissic rocks from the east coast of Lützow-Holm Bay, Antarctica. Mem. Fac. Sci., Kyoto Univ., Ser. Geol. Mineral., **35**, 131–138.

MATSUMOTO, Y., NISHIDA, T., YANAI, K. and KOJIMA, H. (1982): Geology and geologic structure of the northern Ongul Islands and surroundings, East Antarctica. Mem. Natl Inst. Polar Res., Spec. Issue, **21**, 47–70.

MIYASHIRO, A. (1973): Metamorphism and Metamorphic Belts. London, George Allen & Unwin, 492 p.

RAVICH, M. G. and KAMENEV, E. N. (1975): Crystalline Basement of the Antarctic Platform, tr. by N. KANAR. New York, J. Wiley, 582 p.

SHIRAHATA, H. (1983): Lead isotopic composition in the metamorphic rocks from Skarvsnes, East Antarctica. Anatarctic Earth Science, ed. by R. L. OLIVER *et al.* Canberra, Aust. Acad. Sci., 55–58.

SHIRAISHI, K., HIROI, Y. and ONUKI, H. (1984): Orthopyroxene-bearing rocks from the Tenmondai and Naga-iwa Rocks in the Prince Olav Coast, East Antarctica; First appearance of orthopyroxene in progressive metamorphic sequence. Mem. Natl Inst. Polar Res., Spec. Issue, **33**, 126–144.

SUWA, K. (1968): Petrological studies on the metamorphic rocks from the Lützow-Holmbukta area, East Antarctica. 23rd Int. Geol. Congr., **4**, 171–187.

SUZUKI, M. (1982): On the association of orthopyroxene-garnet-biotite found in the Lützow-Holmbukta region, East Antarctica. Mem. Natl Inst. Polar Res., Spec. Issue, **21**, 86–102.

SUZUKI, M. (1983): Preliminary note on the metamorphic conditions around Lützow-Holm Bay, East Antarctica. Mem. Natl Inst. Polar Res., Spec. Issue, **28**, 132–143.

YANAI, K. and UEDA, Y. (1974): Syowa Kiti fukin san ganseki no zettai nendai to sono kôsatsu (Absolute ages and geological investigations on the rocks in the area of around Syowa Station, East Antarctica). Nankyoku Shiryô (Antarct. Rec.), **48**, 70–81.

YANAI, K., KIZAKI, K., TATSUMI, T. and KIKUCHI, T. (1974a): Geological map of East Ongul Island, Antarctica. Antarct. Geol. Map Ser., Sheet 1 (with explanatory text 13 p.). Tokyo, Natl Inst. Polar Res.

YANAI, K., TATSUMI, T. and KIKUCHI, T. (1974b): Geological map of West Ongul Island, Antarctica. Antarct. Geol. Map Ser., Sheet 2 (with explanatory text 5 p.). Tokyo Natl Inst. Polar Res.

YANAI, K., TATSUMI, T., KIKUCHI, T. and ISHIKAWA, T. (1975a): Geological map of Teöya, Antarctica. Antarct. Geol. Map Ser., Sheet 3 (with explanatory text 3 p.). Tokyo, Natl Inst. Polar Res.

YANAI, K., TATSUMI, T. and KIKUCHI, T. (1975b): Geological Map of Ongulkalven Island, Antarctica. Antarct. Geol. Map Ser., Sheet 4 (with explanatory text 3 p.). Tokyo, Natl Inst. Polar Res.

YANAI, K., SHIBATA, K. and SHIRAISHI, K. (1983): Syowa Kiti fukin san henseigan no Rb-Sr nendai (Rb-Sr ages of rocks from Syowa Station). Dai-4-kai Nankyoku Chigaku Shinpojiumu Puroguramu • Kôen Yôshi (Program • Abstr. 4th Symp. Antarct. Geosci.), Tokyo, Natl Inst. Polar Res., 1.

YOSHIDA, M. (1978): Tectonics and petrology of charnockites around Lützow-Holmbukta, East Antarctica. J. Geosci., Osaka City Univ., **21**, 65–152.

YOSHIDA, M. (1979a): Tectonics and metamorphism of the region around Lützow-Holmbukta, East Antarctica. Mem. Natl Inst. Polar Res., Spec. Issue, **14**, 28–40.

YOSHIDA, M. (1979b): Metamorphic conditions of the polymetamorphic Lützow-Holmbukta region, East Antarctica. J. Geosci., Osaka City Univ., **22**, 97–139.

YOSHIDA, M., YANAI, K., YOSHIKURA, S., ISHIKAWA, T. and KANISAWA, S. (1982): Tectonics and microstructure of charnockites around Lützow-Holmbukta, East Antarctica. Antarctic Geoscience, ed. by C. CRADDOCK. Madison, Univ. Wisconsin Press, 511–519.

(Received March 13, 1985)